

Excitation power and temperature dependence of excitons in CuInSe₂

F. Luckert, M. V. Yakushev, C. Faugeras, A. V. Karotki, A. V. Mudryi et al.

Citation: *J. Appl. Phys.* **111**, 093507 (2012); doi: 10.1063/1.4709448

View online: <http://dx.doi.org/10.1063/1.4709448>

View Table of Contents: <http://jap.aip.org/resource/1/JAPIAU/v111/i9>

Published by the [American Institute of Physics](#).

Related Articles

Transport of indirect excitons in a potential energy gradient

Appl. Phys. Lett. **100**, 231106 (2012)

Investigation of energy transfer mechanisms between two adjacent phosphorescent emission layers

J. Appl. Phys. **111**, 113102 (2012)

Excitonic origin of enhanced luminescence quantum efficiency in MgZnO/ZnO coaxial nanowire heterostructures

Appl. Phys. Lett. **100**, 223103 (2012)

Determination of excitonic size with sub-nanometer precision via excitonic Aharonov-Bohm effect in type-II quantum dots

Appl. Phys. Lett. **100**, 213114 (2012)

Luminescence from two-dimensional electron gases in InAlN/GaN heterostructures with different In content

Appl. Phys. Lett. **100**, 212101 (2012)

Additional information on *J. Appl. Phys.*

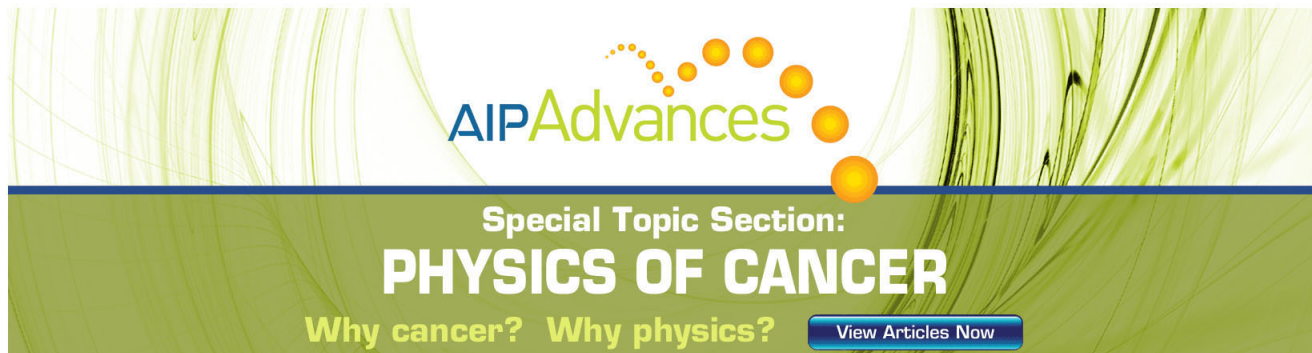
Journal Homepage: <http://jap.aip.org/>

Journal Information: http://jap.aip.org/about/about_the_journal

Top downloads: http://jap.aip.org/features/most_downloaded

Information for Authors: <http://jap.aip.org/authors>

ADVERTISEMENT



AIPAdvances

Special Topic Section:
PHYSICS OF CANCER

Why cancer? Why physics? [View Articles Now](#)

Excitation power and temperature dependence of excitons in CuInSe₂F. Luckert,^{1,a)} M. V. Yakushev,¹ C. Faugeras,² A. V. Karotki,³ A. V. Mudryi,³ and R. W. Martin¹¹*Department of Physics, SUPA, Strathclyde University, Rottenrow 107, G4 0NG Glasgow, United Kingdom*²*Grenoble HMFL, 25 Avenue des Martyrs, BP 166, 38042 Grenoble Cedex 9, France*³*Scientific-Practical Material Research Centre of the National Academy of Science of Belarus, P.Brovki 19, 220072 Minsk, Belarus*

(Received 25 January 2012; accepted 28 March 2012; published online 2 May 2012)

Excitonic recombination processes in high quality CuInSe₂ single crystals have been studied by photoluminescence (PL) and reflectance spectroscopy as a function of excitation powers and temperature. Excitation power dependent measurements confirm the identification of well-resolved A and B free excitons in the PL spectra and analysis of the temperature quenching of these lines provides values for activation energies. These are found to vary from sample to sample, with values of 12.5 and 18.4 meV for the A and B excitons, respectively, in the one showing the highest quality spectra. Analysis of the temperature and power dependent PL spectra from the bound excitonic lines, labelled M1, M2, and M3 appearing in multiplets points to a likely assignment of the hole involved in each case. The M1 excitons appear to involve a conduction band electron and a hole from the B valence band hole. In contrast, an A valence band hole appears to be involved for the M2 and M3 excitons. In addition, the M1 exciton multiplet seems to be due to the radiative recombination of excitons bound to shallow hydrogenic defects, whereas the excitons involved in M2 and M3 are bound to more complex defects. In contrast to the M1 exciton multiplet, the excitonic lines of M2 and M3 saturate at high excitation powers suggesting that the concentration of the defects involved is low. © 2012 American Institute of Physics. [<http://dx.doi.org/10.1063/1.4709448>]

I. INTRODUCTION

CuInSe₂ is a I-III-VI₂ compound semiconductor with the chalcopyrite structure. It exhibits favourable properties for application as an absorber layer in thin film solar cells, such as a direct band gap near 1.05 eV and an absorption coefficient exceeding 10⁵ cm⁻¹. Recently, CuInSe₂-based photovoltaic devices have demonstrated efficiencies of ~20%,¹ which is the highest performance amongst polycrystalline thin-film solar cell technologies. However, this value is still below the 30% predicted theoretically for a single junction solar cell.² Further improvements of the efficiencies will be facilitated by a deeper understanding of the fundamental electronic material properties, in particular the nature of defects.

The chalcopyrite structure of CuInSe₂ involves different chemical bond lengths for Cu-Se and In-Se, which creates a tetragonal distortion.³ This splits the triply degenerated valence band into the three sub-bands A, B, and C. The splitting can be described in terms of the quasicubic model⁴ as the simultaneous influence of the non-cubic crystal-field and the spin-orbit interaction. The tetragonal distortion, τ , is given by $(1 - c/2a)$, where c and a are the lattice constants, and has a small negative value (-0.5%) for the CuInSe₂ single crystals studied here. The negative τ value inverts the valence sub-band symmetry sequence compared to the other chalcopyrites, placing the Γ_{6v} symmetry valence sub-band (A) uppermost and the Γ_{7v} sub-band (B) next. The free excitons corresponding to the A and B valence sub-bands have been observed in

optical reflectivity (OR)^{5,6} and photoluminescence (PL)^{7,8} spectra and their selection rules have been clarified.

The optical properties of CuInSe₂ are controlled by intrinsic defects. Small deviations from the ideal stoichiometry result in a wide variety of such defects,⁹ leading to challenges in their identification.¹⁰

Optical spectroscopy is one of the most powerful tools to study the defects in semiconductors. However, the reported photoluminescence spectra of CuInSe₂ mostly exhibit band-impurity (BI), donor-acceptor pair (DAP), and band-tail related recombination.^{11–15} This suggests that these studies involve material containing high concentrations of defects. If charged, such defects produce potential fluctuations causing broadening of the PL lines. The large spectral widths that result make it difficult to accurately determine the energy levels of the defect within the band gap. In the case of DAP transitions, the involvement of two different defects further complicates their identification. In addition, screening effects caused by high concentrations of charge carriers add to the scatter of measured defect energy levels in the band gap.¹⁰

Study of the optical properties of excitonic states can provide reliable information on the electronic properties^{8,16,17} and the nature of defects.¹⁸ So far, there are only a few reports on CuInSe₂ with clearly resolved excitonic features.^{7,19–21} Temperature and excitation power dependent PL measurements of such excitonic features would provide important information about the free excitons and on the nature of defects associated with the bound excitons.^{22,23} Yakushev *et al.*²⁴ reported an analysis of the temperature and excitation power dependence of the free excitons associated with the A and B valence sub-bands, and of the first three bound excitons.

^{a)}Electronic mail: franziska.luckert@strath.ac.uk.

Although the quality of the CuInSe₂ in that investigation was high enough to resolve the A and B free excitons, the resolution of the different bound exciton lines was limited. In this report, we present a study of CuInSe₂ single crystals of improved structural quality, as demonstrated by PL spectra revealing significantly sharper excitonic lines. A detailed analysis of the excitation power and temperature dependence of the bound and free exciton PL lines is presented.

II. EXPERIMENT

Bulk single crystals of CuInSe₂ were cleaved from the central part of an ingot grown by the vertical Bridgman technique from a near stoichiometric mix of the high purity elements Cu, In, and Se.²⁵ The elemental composition of the crystals, measured by energy dispersive x-ray analysis, was close to ideal stoichiometry (Cu: 24.9, In: 24.9, and Se: 50.2 at. %). Cleaved surfaces of the CuInSe₂ single crystals were examined using temperature and excitation power dependent PL measurements and OR at 4.5 K. Excitation power dependent PL measurements were performed at 4.2 K at the Grenoble High Magnetic Field Laboratory, using a liquid Helium (He) bath cryostat. Optical fibres were used to transport the unpolarised 514 nm line of an Ar⁺ laser to the sample for excitation and the PL to the entrance slits of a 0.5 m spectrometer with an InGaAs array detector. The excitation power was varied from 5 to 30 mW which corresponds to power densities from 16 to 100 W/cm². The liquid He bath cryostat, with the samples surrounded by He vapour, minimises heating of the sample with increasing excitation power, as confirmed by the very small increases in the spectral widths of the PL lines and minimal shift of their spectral positions. The spectral resolution was determined to be 0.14 meV for the excitation power dependent PL.

The OR and temperature dependent PL measurements were performed at the University of Strathclyde. The unpolarised 514 nm line of an Ar⁺ laser was again employed as the PL excitation source; whilst for the OR measurements, a 100 W tungsten halogen lamp was used. The spectral resolution was determined to be 0.07 meV for the OR and 0.2 meV for the temperature dependent PL. The spectral position of the lines was determined with an accuracy of 0.2 meV. In order to take temperature dependent PL spectra, the samples were mounted in a closed-cycle cryostat, allowing the temperature to be varied from 4.5 to 300 K.

III. RESULTS AND DISCUSSION

A. Excitons in CuInSe₂

The near band-edge OR and PL spectra taken at 4.5 and 4.2 K, respectively, are shown in Fig. 1. The OR spectrum, Fig. 1(a), contains two prominent resonances due to the A and B free excitons. This allows the two lines in the PL spectrum appearing at similar energies to be assigned to radiative recombination of free excitons associated with the A and B valence sub-bands. The A and B lines occur at 1.0416 and 1.0451 eV, respectively.

In addition to the free exciton lines, the PL spectrum reveals a number of sharp lines labelled M1 to M7. Some of

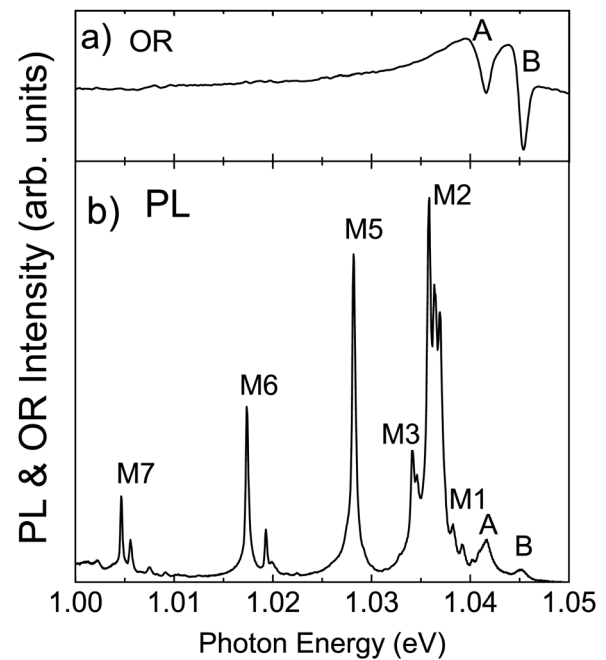


FIG. 1. Near band-edge OR (a) and PL (b) spectra of CuInSe₂ taken at 4.5 and 4.2 K, respectively.

these lines have been observed earlier^{7,20,21,26} and tentatively assigned to ground and excited states of excitons bound to shallow defects. The excitons appear as multiplets and the highest intensity lines are labelled as M1 (1.0383 eV), M2 (1.0358 eV), M3 (1.0341 eV), M5 (1.0282 eV), M6 (1.0174 eV), and M7 (1.0046 eV), using the notations introduced previously.^{21,26} For a detailed analysis of the CuInSe₂ PL spectra, the lines have been fitted with Lorentzian curves using the Levenberg-Marquardt least-square fitting method, as shown in Fig. 2. Generally, the line width of an exciton is determined by processes which limit the time that the exciton spends in the $\mathbf{k} = 0$ state, including phonon scattering.

For weak exciton-phonon coupling, the line shape can be described by a Lorentzian curve, whereas a Gaussian curve occurs where there is strong exciton-phonon coupling.²⁷ In addition, crystal imperfections, impurities, and

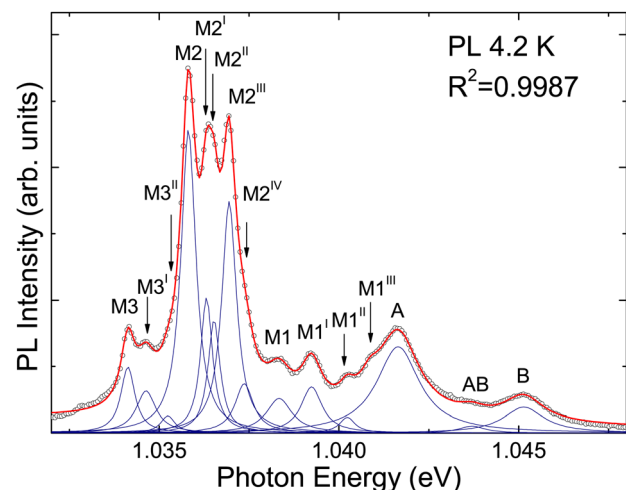


FIG. 2. Fit of the high quality CuInSe₂ spectrum with Lorentzian line shapes (circles-data, blue-individual Lorentzians, and red-fit line).

strain can cause inhomogeneous broadening of the exciton line. If this type of broadening occurs, the observed line will resemble a Gaussian line shape.²⁸ Therefore, the Lorentzian shape of the observed excitonic PL lines suggests low exciton-phonon coupling and a low concentration of crystal imperfections and impurities. A Gaussian line shape of the A and B free exciton lines was reported by Chatrathorn *et al.*⁷ and should be attributed to a high concentration of defects rather than strong exciton-phonon coupling.

Fig. 2 shows that at low temperature the M1, M2, and M3 excitonic multiplets can be decomposed into 4, 5, and 3 peaks, respectively. Lines such as M1^{III}, M2^{III}, M2^{IV}, M3^{II}, and M3^I, which can be seen in Fig. 2, have not been reported previously. Some of the lines, such as M2^{IV} and M3^{II}, are not resolved but without them the overall fit deviates noticeably from the data. Activation energies are not estimated for the weakly resolved peaks but they are included in the excitation power dependence.

In addition, a broad and poorly resolved PL line, labelled as AB in Fig. 2, appears at 1.0435 eV between the two free exciton lines. This PL line could be tentatively associated with an unresolved polaritonic structure of the A and B free excitons. Polariton splitting of the A free exciton has been reported for CuInS₂.²⁹ On the other hand, the AB line could be due to the radiative recombination of a biexciton related to the B free exciton. Biexciton recombination of the A free exciton has been observed in CuInS₂ by Wakita *et al.*³⁰

The accuracy of the obtained fitting parameters as well as the quality of the fit is indicated by the square of the correlation coefficient $R^2 = 0.9987$, whose value is very close to unity.

However, with increasing temperatures the spectral position as well as the width of the excitonic lines changes and it becomes more difficult to obtain accurate fitting information for the less resolved and/or low intensity lines such as AB, M1^{III}, M1^{II}, M2^{IV}; M2^{II}, M3^{II}, and M3^I.

The spectral positions and full width at half maximum (FWHM) of all the lines included in the fit to the PL spectrum in Fig. 2, are shown in Table I. The FWHM of the M lines varies between 0.4 and 0.9 meV, whereas it is about 1.4 meV for the A and B free excitons and 1.8 meV for the AB line. The small value of the FWHM of the M lines suggests that they are of bound excitonic nature.

The assignment of the M lines in Fig. 2 to phonon replica can be ruled out at this point. Tanino *et al.*³¹ reported a minimum phonon energy of 7.44 meV for optical and acoustical phonons in CuInSe₂, whereas the examined spectral region is of about 7.6 meV.

In order to clarify the nature of the excitonic lines shown in Fig. 2, excitation power and temperature dependent PL measurements have been performed.

B. Excitation power dependence

Excitation power dependent PL measurements were performed at liquid Helium temperature for excitation powers ranging from 5 to 30 mW. The spectral position of the PL lines does not depend on the excitation power and changes in the line width are very small. For example, the Lorentzian of

TABLE I. Spectral positions, FWHM, power coefficients k_1 and k_2 (where k_1 corresponds to excitation powers below 20 mW and k_2 to excitation powers above 20 mW for the M2 and M3 excitons), activation energy E_{a1} , process parameter a_1 , and the assignment (FX—free exciton and BX—bound exciton) of the PL lines.

PL line	Energy (eV)	FWHM (meV)	k_1	k_2	E_{a1} (meV)	a_1	Exciton type
B	1.0451	1.4	1.40		18.4	52	FX
AB	1.0435	1.8	1.55				FX
A	1.0416	1.4	1.36		12.5	43	FX
M1 ^{III}	1.0409	0.6	1.61				BX ₁
M1 ^{II}	1.0402	0.5	1.85				BX ₁
M1 ^I	1.0392	0.7	1.50		6.8	11	BX ₁
M1	1.0383	0.9	1.05		7.6	8.6	BX ₁
M2 ^{IV}	1.0374	0.6	1.12				BX ₂
M2 ^{III}	1.0369	0.5	0.88	0.59	7.0	312	BX ₂
M2 ^{II}	1.0365	0.4	0.75	0.64	4.9	97	BX ₂
M2 ^I	1.0363	0.4	0.88	0.60			BX ₂
M2	1.0358	0.5	0.77	0.47	6.0	202	BX ₂
M3 ^{II}	1.0352	0.5	0.93	0.71			BX ₃
M3 ^I	1.0346	0.7	0.66	0.39			BX ₃
M3	1.0341	0.5	0.61	0.39	6.4	615	BX ₃

the M2 excitonic line increases its FWHM from 0.45 to 0.49 meV with excitation densities increasing from 16 to 100 W/cm². This makes it possible to obtain reliable fitting parameters even for the less resolved PL lines.

From the fit of each individual spectrum, the dependencies of the integrated PL intensity (I) of the free and bound excitonic lines, on the laser excitation power P have been obtained, as plotted in Figs. 3 and 4. The dependencies follow the power law $I \sim P^k$. A value of k between 1 and 2 is expected for free exciton transitions since their intensity is

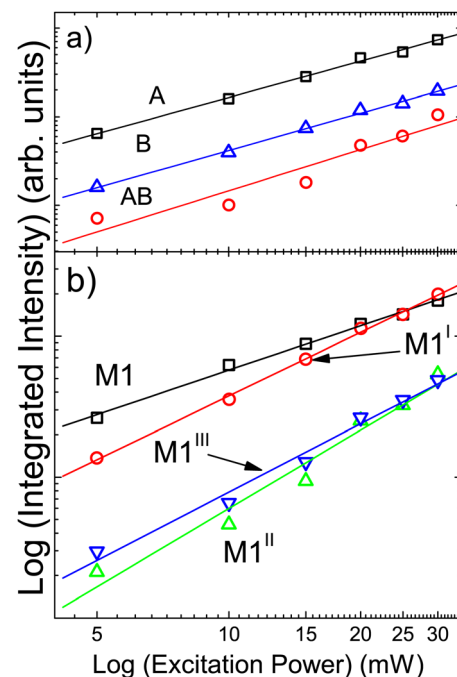


FIG. 3. Experimental dependencies of the A and B free- (a) and M1 bound-exciton PL intensity (b) on the excitation power (symbols) least-square fitted with lines.

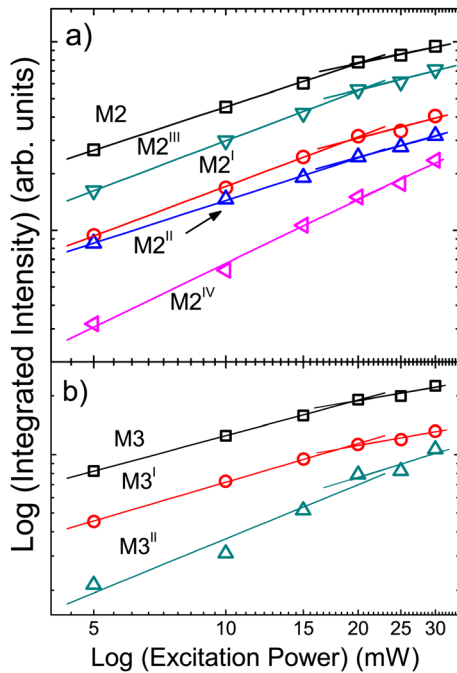


FIG. 4. Experimental dependencies of the M2 (a) and M3 (b) excitons PL intensity on the excitation power (symbols) least-square fitted with lines.

directly proportional to the total number of excitons, which in turn depends on the product of the number of holes and electrons, each of which is proportional to the excitation power P .³² Since bound excitons are in thermal equilibrium with free excitons, the concentration of bound excitons is proportional to that of free excitons.³³ Therefore, values of k between 1 and 2 are also expected for bound exciton transitions, assuming the concentration of defects is high enough and no saturation occurs. For the A and B free excitons, the AB line as well as for the components of the M1 bound exciton, power coefficients $1 < k_1 < 2$ have been determined, as summarised in Table I. The dependence of the integrated intensity on the excitation power of the A, B, AB, and M1 excitonic lines does not show any saturation which confirms that the sample temperature did not rise with increasing excitation and also indicates that the concentration of defects involved in the M1 bound exciton formation is high.

For the bound excitons involved in the M2 and M3 multiplets, with the exception of $M2^{IV}$, the power coefficients are smaller than unity. In addition, Fig. 4 shows a change in the excitation power dependence of the integrated intensity for these lines for powers above about 20 mW. The k coefficients for the M2 and M3 excitonic multiplets are summarised in Table I, where k_1 corresponds to excitation powers below 20 mW and k_2 to excitation powers above 20 mW. Weber *et al.*²³ have reported similar behaviour, namely changes of the slope of the line in the logarithmic plot and $k < 1$, for excitons bound to isoelectronic defects in silicon. These similarities suggest that the M2 and M3 luminescence might originate from excitons bound to isoelectronic defects.

Isoelectronic traps first capture a charge carrier to form an intermediate charged state which then attracts the opposite charge carrier forming a bound exciton. The number of excitons bound to isoelectronic defects is proportional to the

concentration of either the electrons or holes and the number of defects, which produces a linear dependence of PL intensity on excitation power ($k \leq 1$). The change of slope at higher excitation powers can be explained by the saturation of the defects involved. In silicon, these defects are foreign atoms isoelectronically substituting host atoms, binding either holes or electrons to form a state in the forbidden gap.³⁴ For the chalcopyrite compound CuInSe_2 , which is closely related to CuInSe_2 , Krustok *et al.*³⁵ reported emission of excitons bound to defects acting as isoelectronic traps, which were closely situated donor-acceptor pairs acting as neutral centers.

As seen in Fig. 4(a), the excitation power dependence of the $M2^{IV}$ line differs from that of the other excitonic components of M2. A power coefficient $k > 1$ was obtained and $M2^{IV}$ does not saturate above 20 mW. These properties resemble those of the M1 excitons which indicate that $M2^{IV}$ could be another M1 excitonic component or a separate exciton.

Thus our excitation power dependent PL measurements show that the A, AB, and B lines can be associated with free excitons, whereas the M1 components are excitons bound to shallow hydrogenic defects which have a high concentration. With the exception of $M2^{IV}$, the components of the M2 and M3 excitons seem to be bound to more complex defects which may have an isoelectronic nature and whose concentrations are lower than those associated with the M1 exciton.

C. Temperature dependence

The temperature evolution of the PL spectra has been studied for a number of CuInSe_2 single crystals. Figure 5 shows the evolution of the near band-edge PL spectrum with temperature increasing from 5 to 60 K for the highest quality sample. The rapid thermal quenching of the M lines confirms

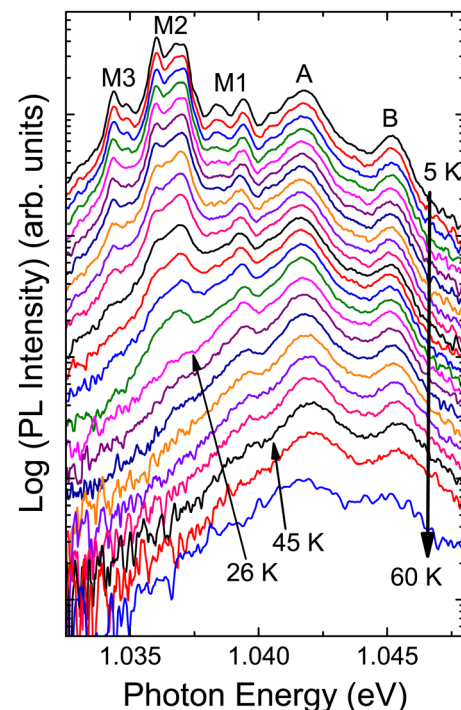


FIG. 5. Evolution of the CuInSe_2 PL spectrum with temperature increasing from 5 to 60 K.

their assignment to the radiative recombination of bound excitons.^{7,20,21,26} In contrast to the M lines, the intensities of the A and B peaks decrease more slowly with increasing temperature and are still present at 60 K. This behaviour confirms the assignment of the A and B lines to free excitons associated with the A and B valence sub-bands.

The different M-lines are seen to quench at different rates. Fig. 5 shows that the M2 and M3 lines have nearly disappeared by about 26 K, whereas the M1 lines are still visible up to about 45 K. The M1 multiplet has a spectral position very close to that of the A free exciton and, if these excitons are associated with the A valence-band, a fast thermal quenching of the M1 lines would be expected. Their slow quenching suggests that a free exciton associated with the B valence sub-band is involved in the formation of the M1 bound exciton, as will be discussed further below.

With increasing temperature, the PL lines change their spectral positions and broaden. Therefore, the following more detailed analysis has been restricted to the most intense and clearly resolved excitonic PL lines: B, A, M1^I, M1, M2^{III}, M2^{II}, M2, and M3.

1. Free excitons

Fig. 6(a) plots the integrated intensity of the A and B free exciton lines versus inverse sample temperature. The temperature quenching of excitonic lines is due to the thermally activated depopulation of the excitonic level and/or to the activation of nonradiative recombination centres. An Arrhenius plot can be used to determine the activation energies E_{a1} of the processes involved. Assuming only one nonradiative

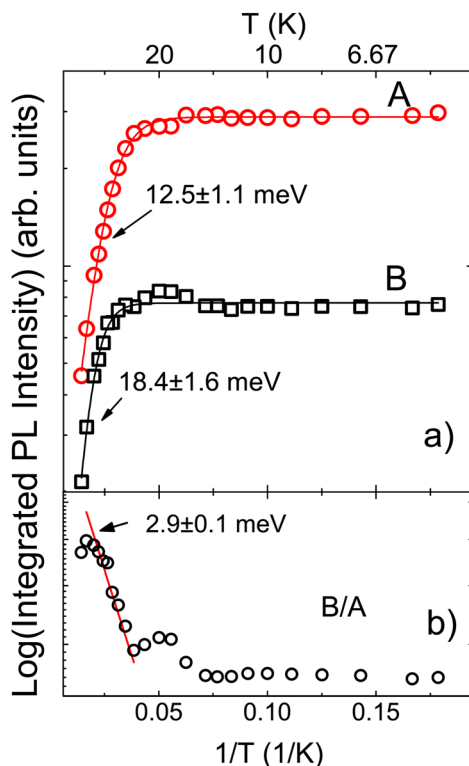


FIG. 6. Arrhenius plot of integrated intensity of the A and B free excitons, fitted with Eq. (1) and the ratio of the integrated intensities of the B and A free excitons (b).

activation channel, the dependence of the integrated intensity I on the temperature T can be described by³⁶

$$I(T) = I_0/[1 + a_1 \exp(-E_{a1}/k_B T)], \quad (1)$$

where I_0 is the emission intensity at the lowest temperature, a_1 is the process rate parameter, E_{a1} is the activation energy, and k_B is the Boltzmann constant. Measurements on other semiconductor materials, such as GaN, have demonstrated values of activation energies for the A exciton that are closely matched to the binding energy of the A exciton.³⁶

The values of E_{a1} and a_1 obtained by the least-square fit of our CuInSe₂ data shown in Fig. 6 are given in Table I. The best fit to the experimental points for the A exciton in this CuInSe₂ single crystal yields an activation energy of 12.5 meV. Chatrathorn *et al.*⁷ determined a value of 12 meV for the activation energy of the A exciton which is in good agreement with this value. However, our temperature quenching analysis of the A free exciton line of lower quality CuInSe₂ crystals resulted in smaller activation energies with a minimum value of about 6 meV. In addition, Yakushev *et al.*²⁴ reported an activation energy of 7.7 meV for a CuInSe₂ sample of a lower quality. Thus, values for E_{a1} for this material are spread over quite a range and are not well matched to the value of the binding energy of the A free exciton, which has been determined as 8.5 meV from the spectral position of the excited states.⁸

The temperature dependence of the integrated intensity of the B exciton has also been fitted using Eq. (1). An activation energy of 18.4 meV was obtained for the highest quality CuInSe₂ single crystal, whereas smaller values down to 7 meV were determined for crystals of lower quality. Literature values of the B exciton activation energy determined from the temperature quenching, range from 7.9 (Ref. 24) to 17 meV.⁷ As with the A exciton, the value of the binding energy of the B exciton (8.4 meV Ref. 8) occurs at a considerably lower energy than E_{a1} for the best crystals.

There are a number of possible explanations for the observed scatter of measured activation energies and the differences from the exciton binding energies. The A and B free excitons are separated by a very small energy splitting (3.3 meV in Fig. 5 and 3.5 meV in Fig. 2) and the thermal transfer of A excitons towards B has not been taken into account in Eq. (1). In addition, the AB peak observed between the A and B exciton lines at low temperatures could have an influence on the E_{a1} values. The M1^{II} and M1^{III} lines can also be seen resolved on the low energy side of the A exciton suggesting the possibility of bound excitons redistributing towards the free excitons. These effects are likely to be the reason for the scatter of the fitted E_{a1} values and the difference of the values measured in the best samples from the exciton binding energy.

An increase of the B exciton intensity above 14 K (~ 0.07 1/K) which is followed by a decrease above 32 K (~ 0.03 1/K) can be seen in Fig. 6(a). This increase could be associated with a thermal transfer of A excitons or/and dissociation of bound excitons towards the B exciton. Fig. 6(b) shows an Arrhenius plot of I_B/I_A , the intensity ratio of the A and B excitons. A significant increase of the B exciton

intensity with respect to A above 23 K (~ 0.04 1/K) can be seen. For temperatures greater than 23 K, the B/A ratio corresponds to a Boltzmann factor $\exp(\Delta/k_B T)$ with an activation energy of $\Delta = 2.9 \pm 0.1$ meV, which is close to the spectral distance between the A and B PL lines. Such an agreement confirms the thermalisation process of A exciton towards B exciton. A similar thermalisation has been reported for GaN (Ref. 36), where the spectral distance between the A and B free excitons is of the order of 7–8 meV.³⁶ As seen in Fig. 6(b), the thermal transfer of A exciton towards the B exciton takes place at temperatures greater than 23 K, which indicates that the observed increase of the B exciton intensity above 14 K is due to the dissociation of bound excitons towards the B free exciton.

2. Bound excitons

The Arrhenius plot of the integrated intensity of the B free exciton in comparison with that of the M1 and M1^I components of the M1 bound exciton is shown in Fig. 7. Using Eq. (1) to describe the experimental points of the M1 and M1^I integrated intensity did not result in a satisfactory fit. A much improved fit is achieved by assuming a dissociation process involving two non-radiative activation channels, as suggested by Bimberg *et al.* for bound excitons in GaAs,³⁷ and described by

$$I(T) = I_0/[1 + a_1 \exp(-E_{a1}/k_B T) + a_2 \exp(-E_{a2}/k_B T)], \quad (2)$$

Fitting the experimental points of the integrated intensities of the M1 and M1^I excitons by Eq. (2) resulted in the two activation energies E_{a1} and E_{a2} , as presented in Table II together with the spectral distances between the M1, M1^I and the A, B free excitons. For temperatures below 32 K (~ 0.03 1/K), activation energies E_{a1} of 7.6 and 6.8 meV have been determined

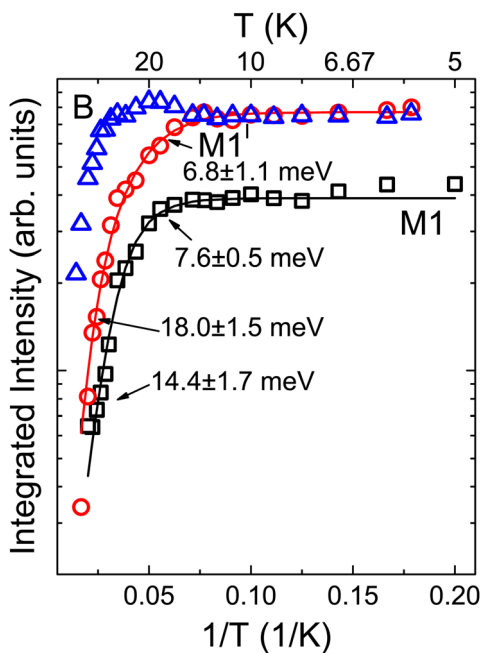


FIG. 7. Arrhenius plot of the integrated PL intensities of the B free exciton and the bound excitons M1 and M1^I, least-square fitted using Eq. (2).

TABLE II. Spectral distances of the M1 and M1^I bound excitons from the A and B excitons, E_{A-BX} and E_{B-BX} , respectively, the activation energies E_{a1} and E_{a2} obtained from the quenching analysis of the integrated PL intensities, using Eq. (2).

PL lines	$E_A - E_{BX}$ (meV)	$E_B - E_{BX}$ (meV)	E_{a1} (meV)	E_{a2} (meV)
M1	3.4	6.8	7.6 ± 0.5	14.4 ± 1.7
M1 ^I	2.4	5.8	6.8 ± 1.1	18.0 ± 1.5

for the M1 and M1^I excitons, respectively. These values are close to those of the spectral distances between the M1 and M1^I and the B free exciton, which suggest that these excitons can be composed of a conduction band electron and a hole from the B valence sub-band. Such an assignment was proposed earlier in Ref. 24. Therefore, the first decrease of the M1 and M1^I lines intensities can be interpreted as thermal detrapping of these excitons towards the B free exciton. This process also leads to the intensity increase of the B exciton at temperatures above 14 K (~ 0.07 1/K) as seen in Fig. 7. The second activation energy E_{a2} has been determined as 14.4 and 18.0 meV for the M1 and M1^I excitons, respectively. This second non-radiative activation channel becomes effective at temperatures above 32 K (~ 0.03 1/K) where the quenching of the PL intensity of the free B exciton is also effective. The dissociation of the B free exciton into one free electron and one free hole would suggest that $E_{a2} = E_{a1} + E_a^B$ with the dissociation energy³⁷ of the B free exciton being $E_a^B = 18.4 \pm 1.6$ meV as described earlier in this paper. The values in Table II show that the sum $E_{a1} + E_a^B$ is larger than E_{a2} for both the M1 and M1^I excitons. However, this

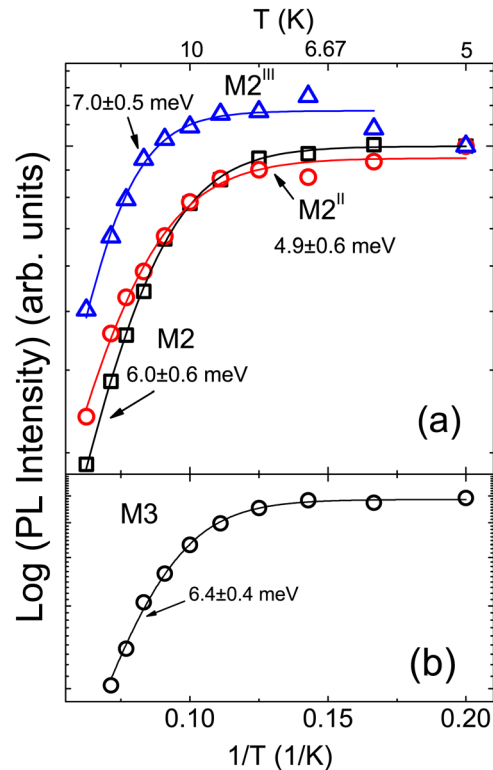


FIG. 8. Arrhenius plot of the integrated PL intensities of the M2 M2^{II} and M2^{III} (a) and M3 (b) bound excitons, least-square fitted using Eq. (1).

TABLE III. Spectral distances of the M2, M2^{II}, M2^{III}, and M3 bound excitons from the A and B excitons, E_{A-BX} and E_{B-BX} , respectively, activation energies E_{a1} obtained from the thermal quenching analysis of the integrated PL intensities and the assignment of the valence sub-band for holes involved in the exciton formation.

PL lines	$E_A - E_{BX}$ (meV)	$E_B - E_{BX}$ (meV)	E_{a1} (meV)	Valence sub-band
M2 ^{III}	4.7	8.1	7.0 ± 0.5	B
M2 ^{II}	5.1	8.4	4.9 ± 0.6	A
M2	5.8	9.2	6.0 ± 0.6	A
M3	7.5	10.8	6.4 ± 0.4	A

difference could be explained by the fact that Eq. (2) does not take into account the interaction between the A and B free excitons.

The integrated intensities of the M2 and M3 excitons are plotted against inverse temperature in Fig. 8. The M2, M2^{II}, M2^{III}, and M3 PL lines have nearly disappeared at temperatures about 26 K. At this temperature, the free excitons have only just started to quench and thus have a very small influence on the quenching of the M2, M2^{II}, M2^{III}, and M3 lines. The experimental data in Fig. 8 can be well fitted with Eq. (1) and the resulting activation energies E_{a1} and process parameter a_1 are summarised in Table I. Table III gives the spectral distances between the M2, M2^{II}, M2^{III}, and M3 lines and the A and B free excitons in comparison with the activation energies.

Table I shows that the process parameters of the M2, M2^{II}, M2^{III}, and M3 lines are significantly greater than those of the M1 and free excitons. Since these parameters can provide indications of the nature of defect involved in the formation of bound excitons,³⁸ it becomes apparent that the nature of defect involved in the M1 bound exciton is different from that of the M2 and M3 bound excitons.

The M2 and M3 excitonic lines have previously been associated with the A free exciton.²⁴ The close comparison between the spectral distances of these lines from the A exciton with the determined activation energies of 6.0 ± 0.6 meV and 6.4 ± 0.4 meV, respectively, agrees with this assignment. In addition, it can be seen from Table III that the M2^{II} line can also be associated with the A free exciton. However, the activation energy obtained for M2^{III} is closer to the spectral distance of this line from the B exciton rather than from the A exciton, which suggests a different nature of M2^{III} compared to the other excitons belonging to the M2 excitonic complex.

IV. CONCLUSION

A study of the excitation power and temperature dependence of the PL of free and bound excitons in high quality CuInSe₂ has been performed. Analysis of the parameters obtained by fitting the PL spectra provides accurate values for the spectral positions and widths of the free and bound excitons.

The OR spectra, together with excitation power dependent PL measurements, identify the A and B lines as free exciton recombination involving holes from the A and B valence

sub-bands, respectively. In addition, it is shown that M1 excitons are bound to shallow defects with a high concentration, whereas most of the M2 (except M2^{IV}) and M3 multiplet excitons appear to be bound to more complex defects with low concentrations. The properties of M2^{IV} resemble those of the M1 excitons suggesting that M2^{IV} could be an additional excitonic component of the M1 multiplet.

The temperature quenching analysis of the A and B PL lines in the highest quality crystal leads to activation energies of 12.5 meV and 18.4 meV for the A and B free excitons, respectively. These values are noticeably larger than the excitonic binding energies and are also found to vary with sample quality. Our temperature quenching analysis revealed a thermal redistribution of A excitons towards the B exciton at temperature above 23 K due to their small energy separation.

Thermal activation energies for the M1, M2, and M3 excitons have also been determined and the assignment of the holes involved in the exciton formation was suggested. It appears that the M1 excitons are composed of a conduction band electron and a B valence band hole. In contrast for the M2^{II}, M2, and M3 excitons the A valence band hole is involved in their formation. For M2^{III}, the assignment of the hole was not conclusive. The exciton corresponding to this line might be different from the other excitons belonging to the M2 excitonic multiplet.

In addition, the analysis of the process parameters of the Arrhenius fit indicated that there is a difference in the nature of defects between the M1 excitons and the M2 and M3 excitons.

ACKNOWLEDGMENTS

The authors would like to thank Dr. M. Leroux (CNRS-CHREA) for many helpful discussions and comments.

This work was supported by the EPSRC (EP/E026451/1), RFBR (10-03-96047 and 11-03-00063), BCFR (F11MC-021), and EC-EuroMagNetII-228043.

¹I. Repins, M. A. Contreras, B. Egaas, C. DeHart, J. Scharf, C. L. Perkins, B. To, and R. Noufi, *Prog. Photovoltaics* **16**, 235 (2008).

²W. Shockley and H. J. Queisser, *J. Appl. Phys.* **32**, 510 (1961).

³J. E. Jaffe and A. Zunger, *Phys. Rev. B* **29**, 1882 (1984).

⁴J. E. Rowe and J. L. Shay, *Phys. Rev. B* **3**, 451 (1971).

⁵J. L. Shay, B. Tell, H. M. Kasper, and L. M. Schiavone, *Phys. Rev. B* **7**, 4485 (1973).

⁶S. Chatrathorn, K. Yoodee, P. Songpongs, and C. Chityuttakan, *Jpn. J. Appl. Phys., Part 1* **39**(Suppl. 39-1), 102 (2000).

⁷S. Chatrathorn, K. Yoodee, P. Songpongs, C. Chityuttakan, K. Sayavong, S. Wongmanerod, and P. O. Holtz, *Jpn. J. Appl. Phys., Part 2* **37**, L269 (1998).

⁸M. V. Yakushev, F. Luckert, C. Faugeras, A. V. Karotki, A. V. Mudryi, and R. W. Martin, *Appl. Phys. Lett.* **97**, 152110 (2010).

⁹S. B. Zhang, S.-H. Wei, A. Zunger, and H. Katayama-Yoshida, *Phys. Rev. B* **57**, 9642 (1998).

¹⁰C. Rincón and R. Márquez, *J. Phys. Chem. Solids* **60**, 1865 (1999).

¹¹P. Yu, *J. Appl. Phys.* **47**, 677 (1976).

¹²F. Abou-Elfotouh, H. Moutinho, A. Bakry, T. J. Coutts, and L. L. Kazmerski, *Sol. Cells* **30**, 151 (1991).

¹³C. Rincón, J. González, and G. Sánchez Pérez, *J. Appl. Phys.* **54**, 6634 (1983).

¹⁴P. Migliorato, J. L. Shay, H. M. Kasper, and W. Sigurd, *J. Appl. Phys.* **46**, 1777 (1975).

- ¹⁵J. Krustok, H. Collan, M. Yakushev, and K. Hjelt, *Phys. Scr.* **T79**, 179 (1999).
- ¹⁶D. G. Thomas and J. J. Hopfield, *Phys. Rev.* **116**, 573 (1959).
- ¹⁷F. Luckert, M. V. Yakushev, C. Faugeras, A. V. Karotki, A. V. Mudryi, and R. W. Martin, *Appl. Phys. Lett.* **97**, 162101 (2010).
- ¹⁸J. J. M. Binsma, L. J. Giling, and J. Bloem, *J. Lumin.* **27**, 55 (1982).
- ¹⁹J. H. Schön and E. Bucher, *Appl. Phys. Lett.* **73**, 211 (1998).
- ²⁰C. Rincon, S. M. Wasim, E. Hernandez, M. A. Arsene, F. Voillot, J. P. Peyrade, G. Bacquet, and A. Albacete, *J. Phys. Chem. Solids* **59**, 245 (1998).
- ²¹A. V. Mudryi, I. V. Bodnar, I. A. Viktorov, V. F. Gremenok, M. V. Yakushev, R. D. Tomlinson, A. E. Hill, and R. D. Pilkington, *Appl. Phys. Lett.* **77**, 2542 (2000).
- ²²A. Bauknecht, S. Siebentritt, J. Albert, Y. Tomm, and M. C. Lux-Steiner, *Jpn. J. Appl. Phys., Part 1* **39**, 322 (2000).
- ²³J. Weber, W. Schmid, and R. Sauer, *Phys. Rev. B* **21**, 2401 (1980).
- ²⁴M. V. Yakushev, R. W. Martin, and A. V. Mudryi, *Phys. Status Solidi C* **6**, 1082 (2009).
- ²⁵R. D. Tomlinson, *Sol. Cells* **16**, 17 (1986).
- ²⁶M. V. Yakushev, Y. Feofanov, R. W. Martin, R. D. Tomlinson, and A. Mudryi, *J. Phys. Chem. Solids* **64**, 2011 (2003).
- ²⁷Y. Toyozawa, *Prog. Theor. Phys.* **20**, 53 (1958).
- ²⁸E. W. Williams and H. B. Bebb, *Transport and Optical Phenomena* (Academic, New York, 1972).
- ²⁹M. V. Yakushev, A. V. Mudryi, I. V. Victorov, J. Krustok, and E. Mellikov, *Appl. Phys. Lett.* **88**, 011922 (2006).
- ³⁰K. Wakita, Y. Ohta, and N. Ohgushi, *Thin Solid Films* **509**, 154 (2006).
- ³¹H. Tanino, T. Maeda, H. Fujikake, H. Nakanishi, S. Endo, and T. Irie, *Phys. Rev. B* **45**, 13323 (1992).
- ³²T. Schmidt, K. Lischka, and W. Zulehner, *Phys. Rev. B* **45**, 8989 (1992).
- ³³A. Yamada, Y. Makita, S. Niki, A. Obara, P. Fons, H. Shibata, M. Kawai, S. Chichibu, and H. Nakanishi, *J. Appl. Phys.* **79**, 4318 (1996).
- ³⁴J. J. Hopfield, D. G. Thomas, and R. T. Lynch, *Phys. Rev. Lett.* **17**, 312 (1966).
- ³⁵J. Krustok, J. Raudoja, and R. Jaaniso, *Appl. Phys. Lett.* **89**, 051905 (2006).
- ³⁶M. Leroux, N. Grandjean, B. Beaumont, G. Nataf, F. Semond, J. Massies, and P. Gibart, *J. Appl. Phys.* **86**, 3721 (1999).
- ³⁷D. Bimberg, M. Sondergeld, and E. Grobe, *Phys. Rev. B* **4**, 3451 (1971).
- ³⁸H. Zimmermann, R. Boyn, and K. Piel, *J. Phys. Condens. Matter* **4**, 859 (1992).